

## Low threshold current density of InAs quantum dash laser on InP (100) through optimizing double cap technique

D. Zhou,<sup>1,2,a)</sup> R. Piron,<sup>1</sup> M. Dontabactouny,<sup>1</sup> O. Dehaese,<sup>1</sup> F. Grillot,<sup>1</sup> T. Batte,<sup>1</sup> K. Tavernier,<sup>1</sup> J. Even,<sup>1</sup> and S. Loualiche<sup>1</sup>

<sup>1</sup>FOTON, INSA-Rennes, 20 avenue des buttes de Cöesmes, 35043 Rennes, France

<sup>2</sup>Department of Electronics and Telecommunications, NTNU, NO-7491 Trondheim, Norway

(Received 4 November 2008; accepted 4 February 2009; published online 24 February 2009)

We report on the uniformity improvement of InAs quantum dashes (QDHs) grown by molecular beam epitaxy on InP (100) through optimizing double cap technique. Broad-area lasers were fabricated with an emission wavelength of 1.58  $\mu\text{m}$ . A threshold current density of 360  $\text{A}/\text{cm}^2$  was achieved for a five stack QDH structure and a cavity length of 1.2 mm. This results from a reduced inhomogeneous broadening (62 meV) and lower internal optical losses (7  $\text{cm}^{-1}$ ). The achievement paves the way toward ultralow threshold semiconductor laser for telecommunications. © 2009 American Institute of Physics. [DOI: 10.1063/1.3088862]

Quantum dash (QDH) lasers on InP substrate are one of the most mature technology for 1.55  $\mu\text{m}$  telecommunications.<sup>1,2</sup> Similar to quantum dot (QD) lasers, some properties such as low threshold current, high differential gain, and small linewidth enhancement factor<sup>3-6</sup> are expected for QDH lasers. Moreover, QDH structure exhibits clear linear polarization, which is an advantage to reduce the bit rate error in device operation. Mode locking has recently been realized by QDH laser at 134 GHz.<sup>7</sup> Ultrafast mode-locked laser requires a short cavity length, and thus low threshold current density ( $J_{\text{th}}$ ) is an important issue. However, low density and high size dispersion of QDH, together with the carrier saturation in the nanostructures, usually lead to low gain and thus high  $J_{\text{th}}$ , as well as in QD lasers. Furthermore, the QDH height or size inhomogeneity is even larger than that of QD, and thus the  $J_{\text{th}}$  of QDH laser is normally several times higher, with similar laser structure design. Besides the increase of areal density of QDHs, several layer stacking is used to increase the active region volume. Furthermore, minimization of the height and/or size dispersion of QDH becomes important in order to achieve ultralow  $J_{\text{th}}$  device. Through the double cap technique,<sup>8</sup> the QDH (QD) height is reduced and the homogeneity is improved. By this mean, ultralow threshold of 170  $\text{A}/\text{cm}^2$  has been measured for an InAs QD laser on InP (311)B.<sup>9</sup> In this letter, we present the investigation and comparison of  $J_{\text{th}}$  in QDH lasers by optimizing the double cap technique, i.e., controlling the energy dispersion and optical losses. Low  $J_{\text{th}}$  of 360  $\text{A}/\text{cm}^2$  is obtained for five-stack QDH laser with a cavity length of 1.2 mm.

The lasers are grown on *n*-type InP (100) substrate by gas source molecular beam epitaxy (MBE). The active region comprises multiple stacked layers with a nominal deposition thickness of 2.1 ML of InAs per layer. The QDH layers are separated by 20 nm barriers of InP lattice-matched  $\text{In}_{0.8}\text{Ga}_{0.2}\text{As}_{0.43}\text{P}_{0.57}$  quaternary ( $Q1.18$ ;  $\lambda_g = 1.18 \mu\text{m}$ ). The active region is centered in a 0.32  $\mu\text{m}$  thick  $Q1.18$  optical waveguide. The core structure is surrounded by InP cladding. The top InP layers is 2.5  $\mu\text{m}$  thick and is capped with a

0.15  $\mu\text{m}$   $p^{++}$ -InGaAs contact layer. Broad area lasers are processed by a conventional lift-off processing technique. The QDH laser stripes are patterned along [011] direction with a width of 100  $\mu\text{m}$ . The laser bars are cleaved into cavities with various lengths and both facets are left uncoated. The laser diodes are electrically pumped by pulsed current with 0.5  $\mu\text{s}$  pulse width and 2 kHz repetition rate.

The growth process uses the double cap technique as well as the control of the arsenic flux to tune the wavelength and to optimize the density.<sup>8</sup> By this mean, the emitting wavelength of the laser can be tuned to the 1.55  $\mu\text{m}$  spectral window. To reduce the photoluminescence (PL) linewidth of QDHs, people adopt many methods. Using AlGaInAs as waveguide avoids As/P exchange and thus full width at half maximum (FWHM) can be obtained  $\sim 50$  meV in InAs/AlGaInAs QDHs.<sup>1</sup> However Al content is not favorable in device fabrication. For InAs/InGaAsP QDHs, reducing the nominal thickness of subsequent QDH layers is developed to control the FWHM increasing during stacking.<sup>2</sup> Alternatively, by double cap technique, we optimize the growth parameters, i.e., first cap thickness and growth interruption time. Two series of samples have been fabricated. In the first group of samples, the QDH layer is capped by a 2.5 nm thick layer of  $Q1.18$ . The growth of this  $Q1.18$  layer is followed by a 60 s growth interruption. This group with a thick  $Q1.18$  layer and a long growth interruption is referred as TK-L. In the second group, the QDH layer is capped by a 2.2 nm thick  $Q1.18$  layer, i.e., a thinner layer than in the first group, and the duration of the following growth interruption is 30 s, i.e., a shorter growth interruption. This second group of samples is referred as TN-S. In both groups of samples, the 20 nm  $Q1.18$  spacer layer is grown after the growth interruption.

Figure 1 is the comparison of normalized PL for the two samples. The measurements are done at room temperature (RT). For the TK-L and TN-S samples, the central PL energy and FWHM are 0.805 eV and 105 meV and 0.797 eV and 62 meV, respectively. The TN-S sample's FWHM is much smaller than that of the TK-L sample. From the PL linewidth point of view, the height dispersion of QDH is strongly reduced in the TN-S sample, which is close to the best value in literature.<sup>1,2</sup>

<sup>a)</sup>Author to whom correspondence should be addressed. Electronic mail: zhoubrave@gmail.com.

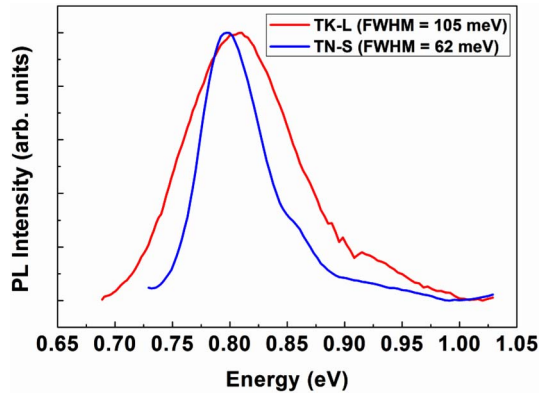


FIG. 1. (Color online) RT PL spectra of a QDH sample with a thicker  $Q1.18$  first capping layer and a longer growth interruption time (TK-L sample) and a QDH sample with a thinner  $Q1.18$  first capping layer and a shorter growth interruption time (TN-S sample).

Figure 2 depicts the threshold current density of QDH lasers  $J_{th}$  versus the inverse cavity length  $1/L$ . The measurements are performed at RT on five-layer stacked QDH lasers. The exponential dependence of  $J_{th}$  with  $1/L$ , extrapolated to zero, yields a threshold current density for infinite cavity length of  $700 \text{ A/cm}^2$  ( $\sim 140 \text{ A/cm}^2$  per QDH layer) for TK-L sample and  $220 \text{ A/cm}^2$  ( $\sim 45 \text{ A/cm}^2$  per layer) for the optimized TN-S sample. For both lasers, the similar slope indicates a similar modal gain factor  $\Gamma g_0$ , resulting from the same waveguide design.

Furthermore, we have measured the light output power as a function of the injection current for these five-stack laser structures. The external differential quantum efficiency is derived from these measurements. The inverse external quantum efficiency  $1/\eta_{ext}$  as a function of cavity length  $L$  is plotted in Fig. 3 for both five-stack QDH TK-L and TN-S lasers. A linear fitting is performed according to  $1/\eta_{ext} = 1/\eta_{int}[1 + \alpha_{int}L/\ln(1/R)]$ , where  $\eta_{int}$  and  $\alpha_{int}$  are the internal differential quantum efficiency and internal optical losses, respectively, and  $R$  is the mirror reflectivity. The internal losses values are thus evaluated to be  $25 \text{ cm}^{-1}$  for TK-L QDH laser and  $7 \text{ cm}^{-1}$  for TN-S QDH laser. These values are comparable to  $19 \text{ cm}^{-1}$  reported in Ref. 1. The reduced internal losses of TN-S sample results from the better control of As/P exchange and probably also from the reducing of In/Ga intermixing due to shorter annealing time. The subtracted internal quantum efficiency of 58% for TN-S

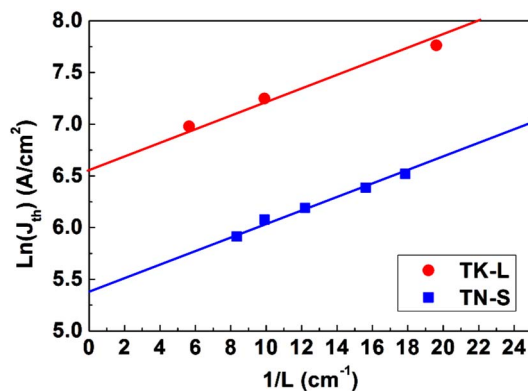


FIG. 2. (Color online)  $J_{th}$  at RT vs the reciprocal cavity length  $1/L$  for five-layer stacked QDH lasers (TK-L/TN-S samples: filled circles/squares). Solid lines are exponential fits of experimental results.

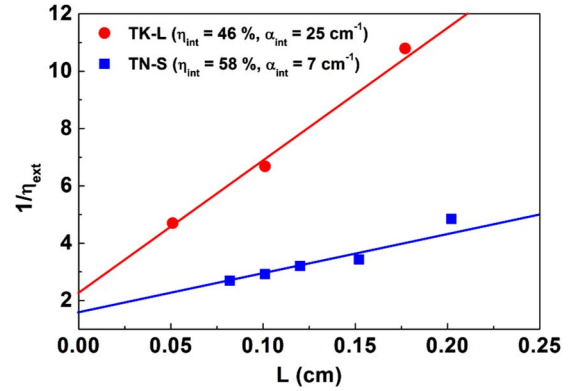


FIG. 3. (Color online) Inverse external quantum efficiency vs cavity length (TK-L/TN-S samples: filled circles/squares).

QDH laser is higher, compared with that of 46% for TK-L QDH laser. Both parameters indicate improved material quality for TN-S cap, i.e., minimization of the strain distribution into the cap layer and the improvement of homogeneity of QDHs. The lower  $\alpha_{int}$  value, as expected for the optimized nanostructure, promotes the decrease of the  $J_{th}$ . Namely, the reduced inhomogeneous broadening of QDHs and the reduced  $\alpha_{int}$  guarantee a lower  $J_{th}$  for the QDH laser through TN-S double cap technique.

Figure 4 depicts the  $J_{th}$  as a function of stack number for TK-L and TN-S QDH lasers with a cavity length of 1.2 mm. Generally, the current density is described as  $J_{th} = J_{QDH} + J_{OCL}$ , where the first component originates from QDH and the second from the optical confinement layer.<sup>10</sup> Neglecting the recombination in the waveguide region (especially for large stack number), the current density will be written as  $J_{th} = J_{QDH} \propto ezN_s/\tau$ , where  $e$  is the unit charge,  $N_s$  is the carrier number in a QDH layer,  $z$  is the stack number of QDH, and  $\tau$  is the carrier lifetime.  $J_{th}$  is therefore linearly dependent on the stack number assuming QDH densities are identical in different layers as described in Ref. 11. The solid lines indicate the quasilinear dependency of  $J_{th}$  on stack number  $z$ .

According to Fig. 4,  $J_{th}$  is much lower for the TN-S QDH laser than for the TK-L one with the same number of layers and cavity length. To explain this, the lasing condition for QDH (QD) laser should be considered. The total number of carriers in QDH ( $zN_s$ ) is the key parameter for laser prop-

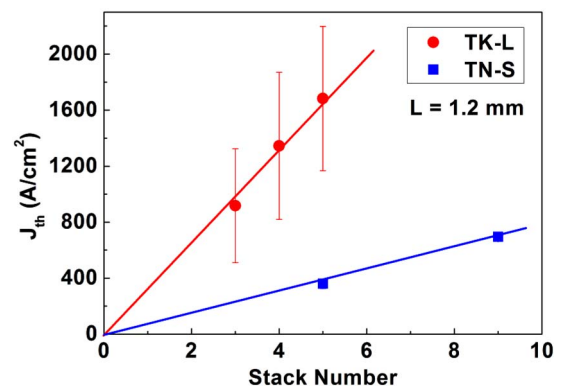


FIG. 4. (Color online) Threshold current density measured at RT as a function of the number of QDH layers for TK-L laser (filled circle) and TN-S laser (filled square) with a cavity length of 1.2 mm. The solid lines are a guide to eyes.

erties. To achieve lasing condition, the total number of carriers in QDH should be larger than a minimum number of carriers ( $N_s^{\text{min}}$ ).  $N_s^{\text{min}}$  is related to the geometrical morphology of QDH and also to their optical properties.  $N_s^{\text{min}}$  could be expressed as  $N_s^{\text{min}} \propto \bar{a}\beta(\Delta\varepsilon)_{\text{inhom}}\tau/\Gamma$ , where  $\bar{a}$  is the average dimension of QDH,  $\beta$  is the optical losses,  $(\Delta\varepsilon)_{\text{inhom}}$  is the energy inhomogeneous broadening of QDH, and  $\Gamma$  is the optical confinement factor for one layer.<sup>10</sup> As the value of  $N_s^{\text{min}}$  is linked to optical losses  $\beta$  and energy inhomogeneous broadening  $(\Delta\varepsilon)_{\text{inhom}}$ , the threshold current density  $J_{\text{th}}$  strongly depends on these factors. The less height or size dispersion of QDHs and/or the lower optical losses, the lower will be the threshold current density. On the other side, a large number of stacked QDH layers must be used to increase the total number of carriers ( $zN_s$ ) to achieve lasing condition when the material quality and structure design are not well optimized.

According to the physical parameters of our samples mentioned above, the  $J_{\text{th}}$  for optimized TN-S QDH lasers are simply estimated to be  $[(7+10) \times 62]/[(25+10) \times 105] \approx 1/3$  of the TK-L ones for the same number of QDH layers and cavity length. This estimation is in accordance with the experimental result of Fig. 4. With as many as nine QDH layers, a  $J_{\text{th}}$  of 690 A/cm<sup>2</sup> is measured, and an ultralow value of 360 A/cm<sup>2</sup> is obtained for five stacked QDH laser structure. Assuming the lasers with lower number of QDH layers could get enough gain to reach lasing, a value of 150 A/cm<sup>2</sup> at RT could be expected for two-stack QDH laser for a cavity length of 1.2 mm, according to the results reported on Fig. 4. In addition, further work could be done to reduce nonradiative recombination processes in the QDH active region to further decrease the  $J_{\text{th}}$ . Lower thresholds and shorter cavity lengths are expected in the future and can ease the realization of ultrafast mode-locked lasers. Moreover, the wavelength emission of the QDH lasers of this work with a cavity length of 1.2 mm is close to 1.58  $\mu\text{m}$ . A further optimization of the thickness of the Q1.18 first capping layer

will allow reaching the 1.55  $\mu\text{m}$  optical telecommunication wavelength.

In conclusion, threshold current densities of quantum dash lasers are studied. The PL FWHM, internal quantum efficiencies, and optical losses are compared. Experimental results show that the laser structure with optimized double cap technique gives a lower threshold current density. This optimized structure allows minimizing the number of carriers required to be present within QDH to reach lasing. Finally, this paves the way for the realization of ultralow threshold devices for optical telecommunications.

The authors would like to thank H. Folliot for the help with PL and N. Chevalier for the useful discussions on MBE growth. This work has been supported by the ePIXnet and Sandie European Networks of Excellence.

<sup>1</sup>F. Lelarge, B. Dagens, J. Renaudier, R. Brenot, A. Accard, F. van Dijk, D. Make, O. Le Gouezigou, J. Provost, F. Poingt, J. Landreau, O. Drisse, E. Derouin, B. Rousseau, F. Pommereau, and G. H. Duan, *IEEE J. Sel. Top. Quantum Electron.* **13**, 111 (2007).

<sup>2</sup>J. P. Reithmaier, G. Eisenstein, and A. Forchel, *Proc. IEEE* **95**, 1779 (2007).

<sup>3</sup>D. Bimberg, N. Kirstaedter, N. N. Ledentsov, Zh. I. Alferov, P. S. Kopev, and V. M. Ustinov, *IEEE J. Sel. Top. Quantum Electron.* **3**, 196 (1997).

<sup>4</sup>D. L. Huffaker, G. Park, Z. Zhou, O. B. Shchekin, and D. G. Deppe, *Appl. Phys. Lett.* **73**, 2564 (1998).

<sup>5</sup>G. T. Liu, A. Stintz, H. Li, K. J. Malloy, and L. F. Lester, *Electron. Lett.* **35**, 1163 (1999).

<sup>6</sup>D. G. Deppe, H. Huang, and O. B. Shchekin, *IEEE J. Quantum Electron.* **38**, 1587 (2002).

<sup>7</sup>C. Gosset, K. Merghem, A. Martinez, G. Moreau, G. Patriarche, G. Aubin, and A. Ramdane, *Appl. Phys. Lett.* **88**, 241105 (2006).

<sup>8</sup>P. Caroff, N. Bertru, C. Platz, O. Dehaese, A. Le Corre, and S. Loualiche, *J. Cryst. Growth* **273**, 357 (2005).

<sup>9</sup>E. Homeyer, R. Piron, F. Grillot, O. Dehaese, K. Tavernier, E. Macé, A. Le Corre, and S. Loualiche, *Jpn. J. Appl. Phys., Part 1* **46**, 6903 (2007).

<sup>10</sup>L. V. Asryan and R. A. Suris, *Semicond. Sci. Technol.* **11**, 554 (1996).

<sup>11</sup>T. Amano, S. Aoki, T. Sugaya, K. Komori, and Y. Okada, *IEEE J. Sel. Top. Quantum Electron.* **13**, 1273 (2007).